© 2022. Published by The Company of Biologists Ltd | Development (2022) 149, dev200231. doi:10.1242/dev.200231

RESEARCH ARTICLE

Kinesin motor KIFC1 is required for tubulin acetylation and actin-dependent spindle migration in mouse oocyte meiosis

Meng-Meng Shan, Yuan-Jing Zou, Zhen-Nan Pan, Hao-Lin Zhang, Yi Xu, Jia-Qian Ju and Shao-Chen Sun*

ABSTRACT

Mammalian oocyte maturation is a unique asymmetric division, which is mainly because of actin-based spindle migration to the cortex. In the present study, we report that a kinesin motor KIFC1, which is associated with microtubules for the maintenance of spindle poles in mitosis, is also involved in actin dynamics in murine oocyte meiosis, co-localizing with microtubules during mouse oocyte maturation. Depletion of KIFC1 caused the failure of polar body extrusion, and we found that meiotic spindle formation and chromosome alignment were disrupted. This might be because of the effects of KIFC1 on HDAC6 and NAT10-based tubulin acetylation, which further affected microtubule stability. Mass spectroscopy analysis revealed that KIFC1 also associated with several actin nucleation factors and we found that KIFC1 was essential for the distribution of actin filaments, which further affected spindle migration. Depletion of KIFC1 leaded to aberrant expression of formin 2 and the ARP2/3 complex, and endoplasmic reticulum distribution was also disturbed. Exogenous KIFC1 mRNA supplement could rescue these defects. Taken together, as well as its roles in tubulin acetylation, our study reported a previously undescribed role of kinesin KIFC1 on the regulation of actin dynamics for spindle migration in mouse oocytes.

KEY WORDS: Kinesin, Oocyte, Meiosis, Tubulin acetylation, Actin, Mouse

INTRODUCTION

Mammalian oocyte meiotic maturation is a unique cell division. After germinal vesicle break down (GVBD), the bipolar meiotic spindle organizes near the center of the oocyte. Accompanied by the migration of the bipolar spindle to the cortex and formation of the actin cap, homologous chromosomes separate and cytokinesis occurs. Ultimately, the oocyte meiosis I completes and a minuscule polar body is extruded, which contributes to the asymmetric division, a unique feature of oocyte maturation (Duan and Sun, 2019). Microtubules and actin filaments play important roles in spindle formation, spindle migration and cytokinesis. Post-translational modifications of tubulin, especially tubulin acetylation, affects microtubule stability and spindle formation. Microtubule-associated proteins (MAPs) are also crucial for the stability of microtubules (Sirajuddin et al., 2014; Song and Brady, 2015). Tubulin acetylation alters the microtubule structure and affects the interaction between microtubules and MAPs (Magiera and Janke, 2014). Acetyltransferases αTAT and NAT10 participate in acetylation of tubulin, whereas deacetylases HDAC6 and Sirt2 are related to deacetylation of tubulin (Coombes et al., 2016; Hubbert et al., 2002; Larrieu et al., 2014; Zhang et al., 2014a). Asymmetric cytokinesis of oocyte meiosis requests precise spindle migration and cleavage furrow formation (Yi et al., 2013b). Actin filaments are widely reported to modulate spindle migration and cytokinesis (Azoury et al., 2008; Holubcová et al., 2013). The Arp2/3 complex, known as an actin nucleator, is demonstrated to regulate oocyte polarization and asymmetric division during mouse oocyte meiosis (Sun et al., 2011; Yi et al., 2011). Formin 2 (Fmn2), a member of formin family, is involved in actin-based spindle positioning and cytokinesis. Spire-type actin nucleators are also found associated with Fmn2 to drive oocyte asymmetric division (Leader et al., 2002; Pfender et al., 2011). In addition, GTPases are reported to be involved in actin assembly in oocytes. For example, RhoA is able to regulate ROCK for phosphorylation of LIMK and cofilin, and further modulates actin dynamics-based spindle migration during mouse and porcine oocyte meiotic maturation (Duan et al., 2014; Zhang et al., 2014b).

Members of the kinesin superfamily are known as the microtubule motor proteins, which are essential for material transport and the maintenance of cellular morphology. Kinesins bind to cargos via their variable tail regions, and move the complex to the destination using the globular motor domain in the head (Hirokawa et al., 2009). The kinesin superfamily is implicated in regulating a range of cellular processes during cell division. For meiosis, Subito, a member of the kinesin 6 family, participates in spindle assembly and stability in *Drosophila* oocytes (Jang et al., 2007). Kif2a and Kif4 are essential for spindle organization and cell cycle regulation in mouse oocytes (Camlin et al., 2017a; Yi et al., 2016). Moreover, many kinesins including Kif3a, Kif6, Kif9, Kif17, and Kif19a have been reported to participate in bipolar spindle assembly, correct microtubule-kinetochore attachments and chromosome separation (Camlin et al., 2017b). And several kinesins, such as Kif18a and Kif26a are found to be related to cell cycle and age-related aneuploidy, which is closely associated with egg quality and embryo development (Camlin et al., 2017b). Therefore, kinesin proteins play indispensable roles during the process of oocyte meiosis and embryo development, which is closely associated with fertility. KIFC1 is a minus end-directed motor protein, which belongs to the kinesin 14 family. KIFC1 is able to regulate DNA synthesis, DNA transport and chromatin maintenance during mitosis, as the conserved nuclear localization signal (NLS) is in the tail domain (Farina et al., 2013; Mazumdar and Misteli, 2005). KIFC1 can also crosslink and transport microtubules, which is crucial for spindle organization (Braun et al., 2009; Cai et al., 2009; Fink et al., 2009; Hentrich and Surrey, 2010). Moreover, KIFC1 is essential for normal spermatogenesis, and its depletion induces aberrant microtubule assembly and apoptosis of spermatogonia/spermatocyte (Hao and

College of Animal Science and Technology, Nanjing Agricultural University, Nanjing 210095, China.

*Author for correspondence (sunsc@njau.edu.cn)

S.-C.S., 0000-0001-5060-1742

Handling Editor: Haruhiko Koseki
Received 28 September 2021; Accepted 18 January 2022

Development (2022) 149, dev200231. doi:10.1242/dev.200231

Yang, 2019). In addition, disturbing the function of KIFC1 causes a rare infertility disease, displaying defective acrosome formation in sperm (Zhi et al., 2016) and aneuploidy in *Drosophila* oocytes (Endow and Komma, 1997; Hatsumi and Endow, 1992; Skold et al., 2005).

Although several studies have reported the roles of KIFC1 on microtubule dynamics in mitosis, its roles in mouse oocyte meiosis still remain unknown. In the present study, we investigated the roles of KIFC1 in mouse oocyte meiosis by depleting KIFC1 expression and observing the rescue approach. Besides its role in microtubule dynamics, our results deciphered a previously undescribed role of KIFC1 in actin-mediated spindle migration and actin cap formation during mouse oocyte maturation.

RESULTS

Expression and localization of KIFC1 in mouse oocyte meiosis

We first examined KIFC1 expression levels at different maturation stages during mouse oocyte meiosis. We collected mouse oocytes after culture of 0, 4, 8 and 12 h, which represented the stages of the germinal vesicle (GV), GVBD, metaphase I (MI) and metaphase II (MII), respectively. Our results showed that KIFC1 was expressed at all the meiosis stages in mouse oocytes (Fig. 1A). We then examined KIFC1 localization at these stages of mouse oocyte meiotic maturation. After GVBD, KIFC1 accumulated around the chromosomes and localized with the spindle/central spindle in the MI, anaphase-telophase I (ATI) and MII stages (Fig. 1B). To confirm this, we co-stained tubulin and KIFC1 and the results showed that KIFC1 co-localized with microtubules at MI and ATI stages (Fig. 1C). To further verify whether the localization of KIFC1 was microtubule-dependent, we disturbed the microtubules by nocodazole and taxol treatment, which could promote the depolymerization and polymerization of microtubules, respectively. Upon nocodazole treatment, KIFC1 dispersed into the cytoplasm as the microtubules were depolymerized and the spindle was disassembled (Fig. 1D). Upon taxol treatment, the microtubules were polymerized in the oocyte cytoplasm and KIFC1 still localized at the microtubules including asters in MI oocytes (Fig. 1E). We also produced exogenous Myc-KIFC1 mRNA and injected into the oocytes to detect the subcellular localization pattern of KIFC1 in oocytes. Similar to antibody staining, we showed that Myc-KIFC1 was co-localized with the microtubules at MI, which confirmed the successful translation of Myc-KIFC1 mRNA in the oocytes (Fig. 1F).

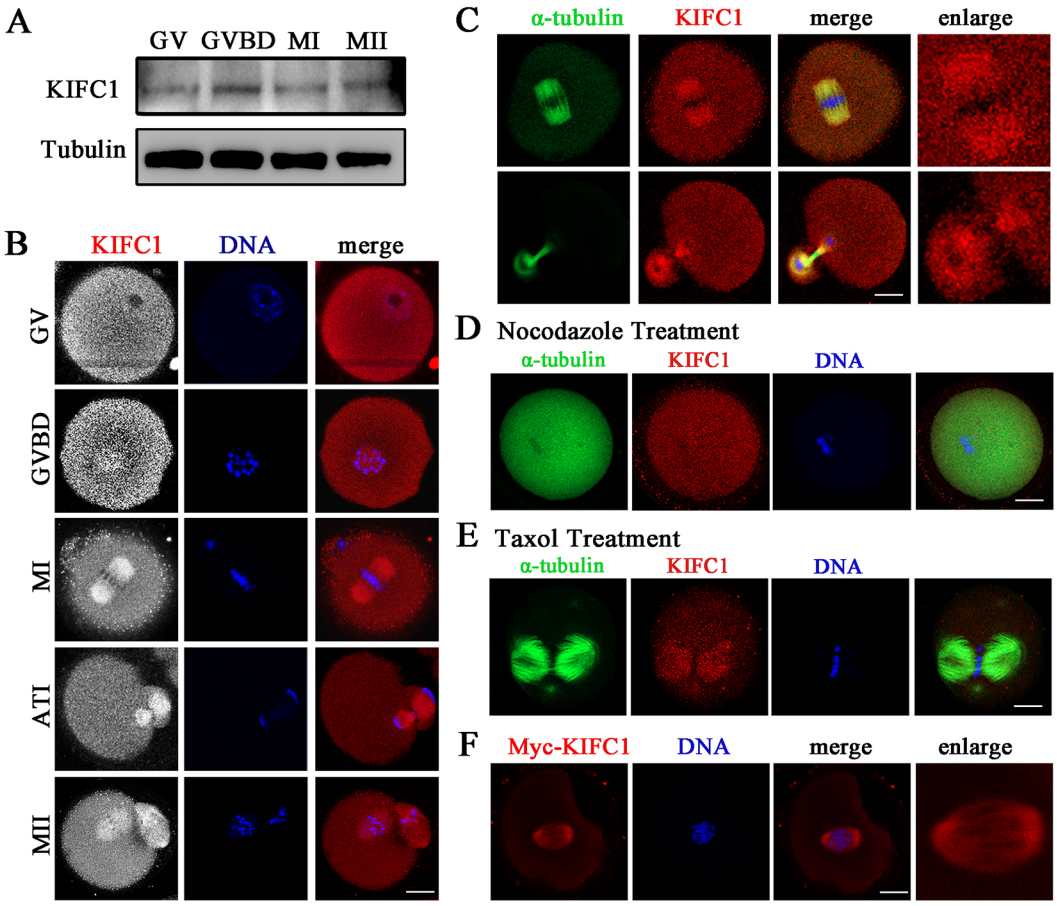

Fig. 1. Expression and localization of KIFC1 in mouse oocyte meiosis. (A) Protein levels of KIFC1 in oocytes at GV (0 h), GVBD (4 h), metaphase I (MI; 8 h), and metaphase II (MII; 12 h) stages were examined by western blot. Each group contained 250 oocytes. Tubulin was set as the control. (B) Mouse oocytes at GV, GVBD, MI, ATI and MII stages were immunolabeled with mouse anti-KIFC1 antibody. KIFC1 was distributed at the spindle in the oocytes at different stages. Red, KIFC1; blue, DNA. (C) Co-staining of KIFC1 (red) and α-tubulin (green) in oocytes cultured to the MI and ATI stages. DNA (blue) was counterstained with Hoechst 33342. (D) Subcellular localization of KIFC1 after nocodazole treatment in mouse oocyte of MI. Green, α-tubulin; red, KIFC1; blue, DNA. (E) Subcellular localization of KIFC1 after taxol treatment in mouse oocyte of MI. Green, α-tubulin; red, KIFC1; blue, DNA. (F) The localization of Myc-KIFC1 protein after Myc-KIFC1 mRNA injection in the oocytes. Myc-KIFC1 was observed on the spindle. Red, Myc-KIFC1; blue, DNA. Scale bars: 20 µm.

Development (2022) 149, dev200231. doi:10.1242/dev.200231

KIFC1 is essential for mouse oocyte meiotic maturation

We next examined the functions of KIFC1 in mouse oocytes using morpholino injection and the KIFC1-specific inhibitor AZ82 (10 µM). After morpholino injection, the expression of KIFC1 was significantly decreased (control-MO 1 versus KIFC1-MO 0.10, $P<0.001$) (Fig. 2A). After culturing for 4 h, we found that KIFC1 suppression had no significant effect on the GVBD rate, indicating that KIFC1 did not affect meiosis resumption [control (DMSO) 71.67±2.96%, $n=112$, versus 10 µM AZ82 76.67±4.05%, $n=127$, not significant; control-MO 60.67±1.76%, $n=114$, versus KIFC1-MO 52.67±3.84%, $n=127$, not significant] (Fig. 2B). However, there was a significant effect on the first polar body extrusion of KIFC1 after the morpholino injection and AZ82 treatment (Fig. 2C). Statistical analysis showed that the percentage of the polar body extrusion in KIFC1 suppression oocytes was significantly reduced compared with control oocytes [control (DMSO) 71.84±3.92%, $n=134$, versus 10 µM AZ82 45.98±3.90%, $n=147$, $P<0.05$; control-MO 69.36±3.13%, $n=121$, versus KIFC1-MO 29.01±6.65%, $n=126$, $P<0.001$] (Fig. 2D). After mRNA injection, the protein expression of KIFC1 also significantly increased compared with the morpholino injection group, which was confirmed by the band intensity analysis (control-MO 1 versus rescue 1.09, not significant; control-MO versus KIFC1-MO 0.22, $P<0.01$) (Fig. 2E). The injection of Myc-KIFC1 mRNA rescued the defects of the polar body extrusion caused by morpholino injection (Fig. 2F). Myc-KIFC1 mRNA injection effectively rescued the rate of polar body extrusion (control-MO 71.33±0.88%, $n=137$, versus KIFC1-MO 27.33±1.45%, $n=97$, $P<0.01$; control-MO versus rescue 61.33±1.45%, $n=69$, $P<0.01$) (Fig. 2G). These results indicated that KIFC1 was essential for mouse oocyte meiotic maturation and its depletion caused polar body extrusion defects.

KIFC1 regulates spindle formation and chromosome alignment in mouse oocyte meiosis

Given the localization pattern of KIFC1 on microtubules, we speculated that KIFC1 might have a microtubule-related function, so we next investigated spindle morphology after KIFC1 depletion.

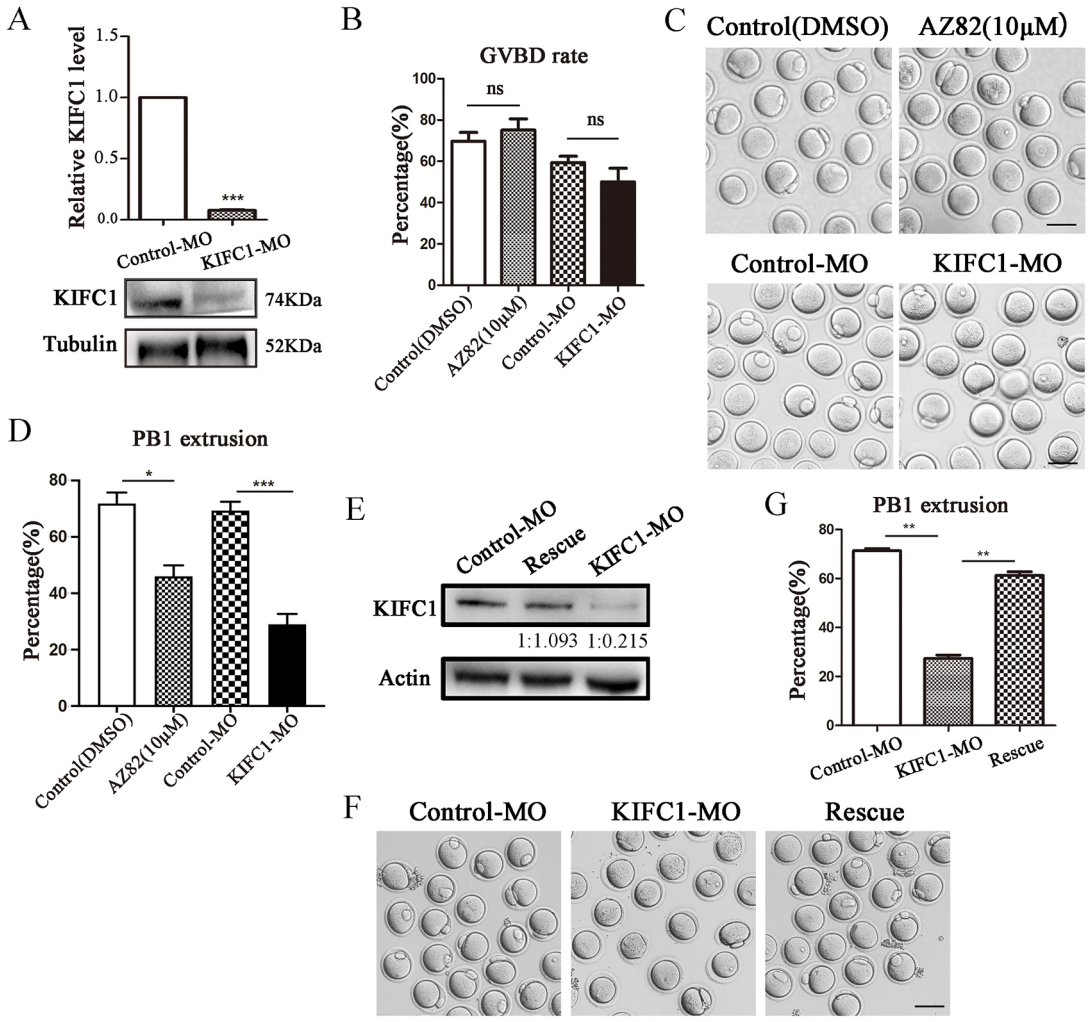

Fig. 2. KIFC1 is essential for mouse oocyte meiotic maturation. (A) Western blot analysis showed a significant decrease of KIFC1 expression in the morpholino-injection oocytes compared with the control oligo-injection oocytes. Each group contained 250 GV oocytes. (B) Treatment with AZ82 or morpholino injection had no effect on GVBD rates in mouse oocytes. (C) Representative images of polar body extrusion in the control, KIFC1-inhibited and KIFC1 morpholino-injection oocytes. (D) KIFC1 suppression significantly decreased the percentages of polar body extrusion in mouse oocytes. (E) The expression of KIFC1 was significantly increased compared with the KIFC1 knockdown group after injection of Myc-KIFC1 mRNA. (F) Representative images of polar body extrusion in the control-MO, KIFC1-MO and rescue oocytes. (G) The polar body extrusion defects caused by KIFC1 knockdown was rescued by the supplementation of KIFC1 mRNA. Data are mean±s.e.m. *$P<0.05$, **$P<0.01$, ***$P<0.001$ (paired two-tailed Student's *t*-test). ns, not significant. Scale bars: 80 µm.

Development (2022) 149, dev200231. doi:10.1242/dev.200231

As shown in Fig. 3A, we found that depleting KFC1 expression or disturbing KIFC1 activity both significantly disrupted spindle assembly. Oocytes in the control group had typical barrel-shape spindles and accurate alignment of chromosomes at MI stage. In contrast, oocytes in the treated group had significant aberrant spindles and severely misaligned chromosomes. These aberrant spindles displayed multipolar spindles with more than two poles or distorted spindles with several scattered chromosomes. Statistical analysis showed that the percentage of abnormal spindles in the KIFC1 knockdown and inhibition group was significantly higher than that in the control group [control (DMSO) 22.43±4.97%, n=84, versus 10 µM AZ82 58.89±1.70%, n=97, P<0.05; control-MO 26.88±1.20%, n=71, versus KIFC1-MO 48.64±2.58%, n=86, P<0.05] (Fig. 3B). Meanwhile, the percentage of misaligned

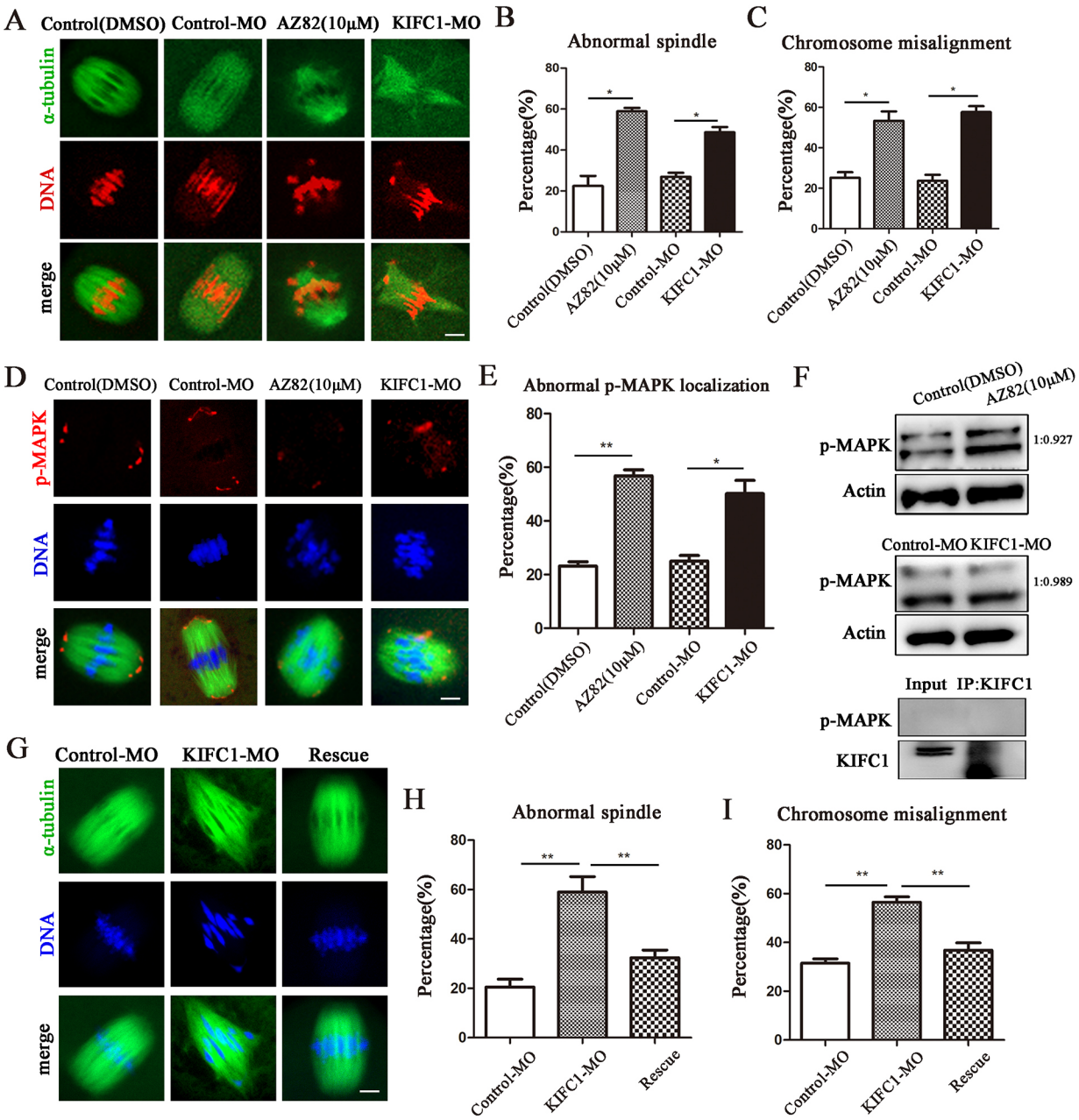

Fig. 3. KIFC1 regulates spindle formation and chromosome alignment in mouse oocyte meiosis. (A) Suppression of KIFC1 led to chromosome misalignment and formation of abnormal spindles in metaphase I (MI) oocytes. DNA and α-tubulin are shown in red and green, respectively. (B) The rate of spindle disorganization after AZ82 treatment or morpholino injection. (C) The rate of chromosome misalignment after AZ82 treatment or morpholino injection. (D) Localization of p-MAPK in mouse oocytes of MI after KIFC1 suppression. Oocytes after 8 h culturing were stained for p-MAPK (red), α-tubulin (green) and DNA (blue). (E) The rate of abnormal p-MAPK localization of MI oocytes in each group. (F) Western blot analysis of p-MAPK expression in KIFC1 suppression and control oocytes of MI: the results showed no difference between each group. Co-IP results showed that KIFC1 was not correlated with p-MAPK. (G) Myc-KIFC1 mRNA injection rescued chromosome misalignment and abnormal spindles caused by KIFC1 knockdown. Green, α-tubulin; blue, DNA. (H) The rate of spindle abnormality was significantly increased in KIFC1-MO oocytes compared with control oocytes, and it was reduced in Myc-KIFC1 mRNA-injected oocytes compared with KIFC1-MO oocytes. (I) The rate of chromosome misalignment was significantly increased in KIFC1-MO oocytes compared with control oocytes, and it was reduced in Myc-KIFC1 mRNA-injected oocytes compared with KIFC1-MO oocytes. Data are mean±s.e.m. *P<0.05, **P<0.01 (paired two-tailed Student's t-test). Scale bars: 5 µm.

Development (2022) 149, dev200231. doi:10.1242/dev.200231

chromosomes in the KIFC1 knockdown or inhibition group was significantly higher than that in the control group [control (DMSO) 25.17±2.76%, *n*=64, versus 10 µM AZ82 53.33±4.63%, *n*=87, *P*<0.05; control-MO 23.72±2.89%, *n*=76, versus KIFC1-MO 57.65±2.92%, *n*=82, *P*<0.05] (Fig. 3C). MAPK is widely known as a typical kinase with bipolar localization that is required for proper tubulin nucleation and spindle assembly during oocyte meiosis (Fan and Sun, 2004). As shown in Fig. 3D, p-MAPK was localized at the spindle poles in control MI oocytes; however, it dispersed from the disrupted spindles in the KIFC1 knockdown or inhibition group. Statistical analysis showed that the percentage of abnormal p-MAPK localization in KIFC1 suppression group was significantly higher than that in the control group [control (DMSO) 23.20±1.60%, *n*=74, versus 10 µM AZ82 56.76±2.27%, *n*=67, *P*<0.01; control-MO 25.05±2.04%, *n*=86, versus KIFC1-MO 50.15±4.93%, *n*=81, *P*<0.05] (Fig. 3E). However, there was no difference in the expression of p-MAPK in the morpholino injection and inhibition group [control (DMSO) 1 versus 10 µM AZ82 0.93, not significant; control-MO 1 versus KIFC1-MO 0.99, not significant]. The results of co-immunoprecipitation (co-IP) also showed that there was no mutual relationship between KIFC1 and p-MAPK (Fig. 3F). We found that spindle abnormality and chromosome misalignment could be partly rescued by Myc-KIFC1 mRNA injection (Fig. 3G). The high rate of abnormal spindles and misaligned chromosomes caused by morpholino injection could be ameliorated by Myc-KIFC1 mRNA injection (abnormal spindles: control-MO 20.50±3.21%, *n*=142, versus KIFC1-MO 58.99±6.22%, *n*=73, *P*<0.01, control-MO versus rescue 32.34±3.18%, *n*=75, *P*<0.01; chromosome misalignment: control-MO 31.48±1.85%, *n*=102, versus KIFC1-MO 56.51±2.22%, *n*=107, *P*<0.01, control-MO versus rescue 36.81±3.03%, *n*=79, *P*<0.01) (Fig. 3H,I). These results suggested that KIFC1 had a crucial role in spindle formation and chromosome alignment in mouse oocytes.

KIFC1 regulates tubulin acetylation levels in mouse oocyte meiosis

We then detected the acetylation levels of α-tubulin by immunostaining to evaluate microtubule stability. We found that the tubulin acetylation level was significantly increased in both morpholino injection and inhibition groups (Fig. 4A). Rates of acetylated α-tubulin (ac-tubulin) fluorescence intensity-increased oocytes in treated groups were significantly higher than those of control groups [control (DMSO) 35.55±2.22%, *n*=74, versus 10 µM AZ82 64.82±8.07%, *n*=67, *P*<0.05; control-MO 35.92±4.37%, *n*=73, versus KIFC1-MO 67.22±4.34%, *n*=62, *P*<0.05] (Fig. 4B). To explore the regulatory mechanism of KIFC1 on tubulin acetylation and spindle assembly, we performed mass spectrometry analysis and found several acetylated transferases (Fig. 4C). Through co-IP experiments, we found that acetylase NAT10 and deacetylase HDAC6 were combined with KIFC1 spatially (Fig. 4D). We subsequently detected the expression level of acetyltransferase NAT10 and deacetylase HDAC6. Analysis of the band intensity showed that HDAC6 expression decreased and the expression of NAT10 increased in the MO-injection group, with a significantly increased protein expression of ac-tubulin (NAT10: control-MO 1 versus KIFC1-MO 1.53, *P*<0.01; HDAC6: control-MO 1 versus KIFC1-MO 0.76, *P*<0.05; ac-tubulin: control-MO 1 versus KIFC1-MO 2.12, *P*<0.01) (Fig. 4E). We also found that increased fluorescence intensity of ac-tubulin can be significantly rescued by Myc-KIFC1 mRNA injection (control-MO 1, *n*=82, versus KIFC1-MO 1.51±0.08, *n*=93, *P*<0.05; control-MO versus rescue 0.97±0.05, *n*=87, *P*<0.05) (Fig. 4F,G). Moreover, the protein expression of ac-tubulin also significantly decreased compared with the morpholino injection group, which also confirmed by the band intensity analysis (control-MO 1 versus rescue 1.04, not significant; control-MO versus KIFC1-MO 1.75, *P*<0.01) (Fig. 4H). The results indicated that KIFC1 regulated spindle organization through its effects on tubulin acetylation during mouse oocyte maturation.

KIFC1 regulates actin dynamics and spindle migration in mouse oocyte meiosis

To explore the regulatory mechanism of KIFC1 on oocyte maturation, we performed mass spectrometry analysis and found several actin-related proteins such as the ARP2/3 complex, profilin and cofilin associated with KIFC1 (Fig. 5A). This prompted us to explore the function of KIFC1 on actin. As shown in Fig. 5B, oocytes in the control group had high actin filament signals at the oocyte cytoplasm and cortex. In contrast, oocytes in KIFC1 MO-injection and inhibition groups had obviously decreased actin filament signals. Statistical analysis showed that actin fluorescence intensity of the cytoplasm in the KIFC1 knockdown and inhibition oocytes was significantly lower than that in the control oocytes [control (DMSO) 1, *n*=73, versus 10 µM AZ82 0.72±0.03, *n*=68, *P*<0.001; control-MO 1, *n*=84, versus KIFC1-MO 0.85±0.03, *n*=62, *P*<0.01] (Fig. 5C). Moreover, oocytes in KIFC1 suppression groups also had significantly lower actin filament signals at the oocyte cortical area [control (DMSO) 1, *n*=76, versus 10 µM AZ82 0.66±0.03, *n*=82, *P*<0.001; control-MO 1, *n*=64, versus KIFC1-MO 0.85±0.03, *n*=68, *P*<0.01] (Fig. 5D).

Spindle migration in oocytes was next detected, as it was an actin-based cellular process in oocytes. We examined the spindle position after 9 h of culture. As shown in Fig. 5E, the meiotic spindle migrated to the cortex in the majority of oocytes in the control group, whereas most spindles in the KIFC1-depleted oocytes were arrested in the center of the cytoplasm. To quantitatively determine the spindle position in oocytes after KIFC1 knockdown, we defined D as the distance from the near-end of the spindle pole to the cortex and defined L as the distance from the far-end of the spindle pole to the cortex (Fig. 5F). The D/L ratio was significantly higher in the treated group than that in the control group [control (DMSO) 0.25±0.06, *n*=57, versus 10 µM AZ82 0.82±0.06, *n*=62, *P*<0.05; control-MO 0.36±0.02, *n*=68, versus KIFC1-MO 0.77±0.01, *n*=64, *P*<0.01]. The formation of the actin cap is a predominant feature of oocyte polarization, which is disturbed by the failure of spindle migration. The actin cap was clearly observed in oocytes of the control group at late MI stage; however, treated oocytes missed the typical actin caps (Fig. 5G). The quantitative analysis showed that the percentage of oocytes with actin cap in the KIFC1 suppression group was significantly lower than that in the control group [control (DMSO) 74.56±1.25%, *n*=134, versus 10 µM AZ82 39.34±0.34%, *n*=87, *P*<0.01; control-MO 73.09±1.75%, *n*=81, versus KIFC1-MO 45.60±4.40%, *n*=96, *P*<0.05] (Fig. 5H). We also performed rescue experiment by Myc-KIFC1 mRNA injection and found notable recovery of actin signals in both cytoplasm and cortex (Fig. 5I), which could be confirmed by fluorescence intensity analysis (cytoplasm: control-MO 1, n=72, versus KIFC1-MO 0.71±0.03, *n*=63, *P*<0.05; KIFC1-MO versus rescue 0.94±0.03, *n*=74, *P*<0.05; cortex: control-MO 1, *n*=89, versus KIFC1-MO 0.59±0.05, *n*=92, *P*<0.01; KIFC1-MO versus rescue 0.96±0.01, *n*=83, *P*<0.01) (Fig. 5J). These data indicated that KIFC1 played a crucial role in spindle migration, which acts in an actin-dependent manner during oocyte meiotic maturation.

Development (2022) 149, dev200231. doi:10.1242/dev.200231

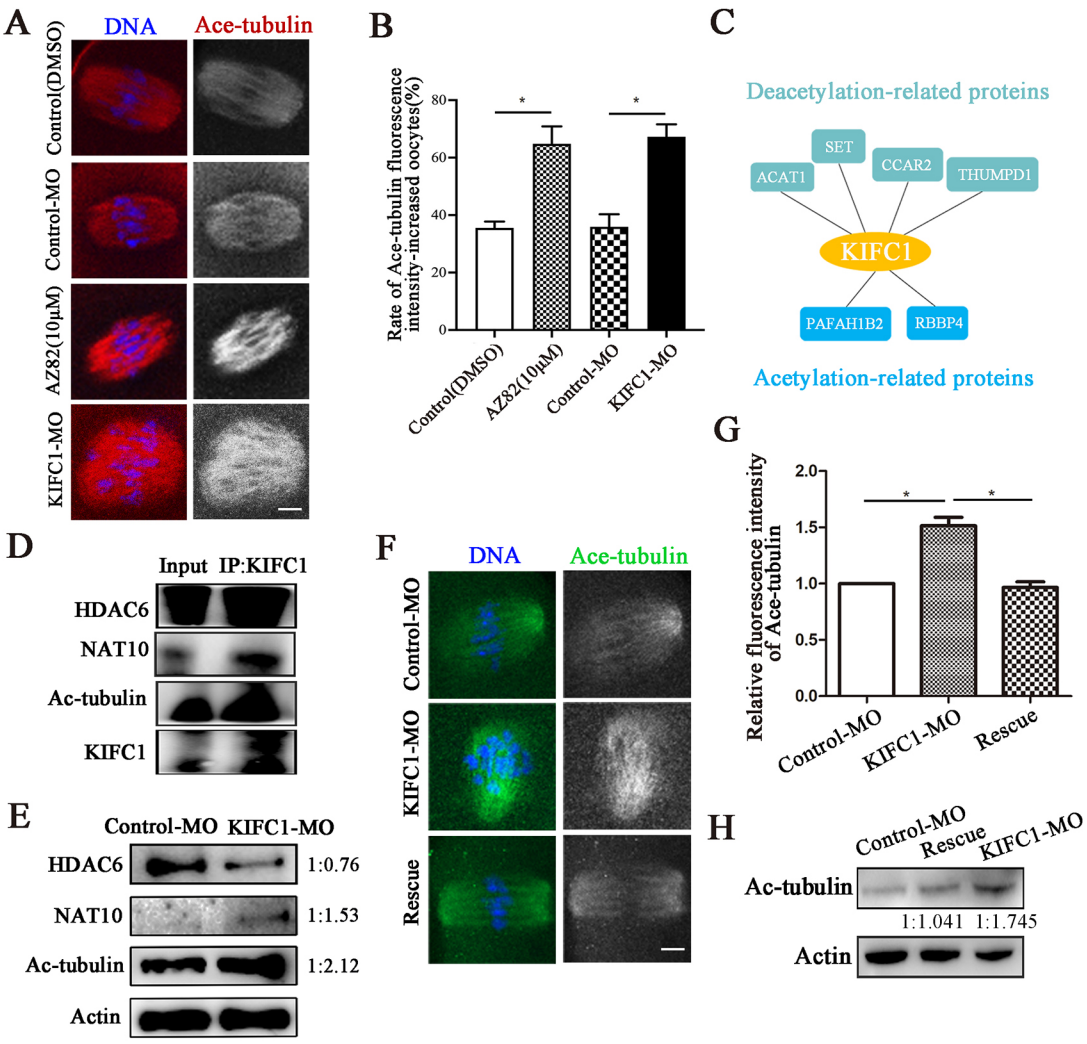

Fig. 4. KIFC1 affects α-tubulin acetylation levels in mouse oocyte meiosis. (A) Representative images of acetylated α-tubulin (Ace-tubulin; red) in control and treated oocytes of metaphase I (MI). Blue, DNA. (B) Quantitative analysis of acetylated α-tubulin fluorescence intensities in oocytes of both groups. (C) Screening acetylation-related proteins and deacetylation-related proteins correlated with KIFC1 by mass spectrometry analysis. (D) Co-IP results showed that KIFC1 was correlated with acetylase NAT10, deacetylase HDAC6 and acetylated α-tubulin (ac-tubulin). (E) The expression level of acetylated α-tubulin was increased in MI-stage oocytes of the KIFC1 knockdown group. Meanwhile, KIFC1 knockdown significantly increased expression of NAT10 and decreased expression of HDAC6 in mouse oocytes. (F) Increased fluorescence intensity of acetylated α-tubulin in KIFC1-MO oocytes can be significantly rescued by Myc-KIFC1 mRNA injection. Green, ac-tubulin; blue, DNA. (G) The fluorescence intensity of acetylated α-tubulin after Myc-KIFC1 mRNA injection was significantly decreased compared with the KIFC1-MO group. (H) The expression of acetylated α-tubulin was significantly recovered compared with the control group after injection of Myc-KIFC1 mRNA. Data are mean±s.e.m. *P<0.05 (paired two-tailed Student's t-test). Scale bars: 5 µm.

KIFC1 regulates actin nucleator functions in mouse oocytes

Through immunoprecipitation (IP), we found that KIFC1 had correlation with actin-related proteins ARP2, Fmn2 and N-WASP (also known as Wasl), but not Daam1, cofilin and profilin (Fig. 6A). In KIFC1-depleted oocytes, the expression level of ARP2, Fmn2 and N-WASP was reduced (ARP2: control-MO 1 versus KIFC1-MO 0.68, P<0.01; Fmn2: control-MO 1 versus KIFC1-MO 0.36, P<0.01; N-WASP: control-MO 1 versus KIFC1-MO 0.72, P<0.05) (Fig. 6B). We showed that ARP2 accumulated in the cortical region that overlaid the chromosomes, which was coincident with the actin cap in control oocytes, whereas the polarized ARP2 signals were undetectable in KIFC1-depleted oocytes (Fig. 6C). Quantitative analysis demonstrated that ARP2 cap formation at the cortex was significantly reduced in KIFC1 suppression oocytes compared with that in the control oocytes (control-MO 70.37±3.70%, n=89, versus KIFC1-MO 43.01±5.31%, n=83, P<0.01) (Fig. 6D). We also examined the localization of Fmn2 in oocytes after KIFC1 depletion. The immunofluorescence signal of Fmn2 distributed on the spindle was obviously reduced after MO injection (Fig. 6E). Quantitative analysis demonstrated that the rate of abnormal localization of Fmn2 was significantly increased in KIFC1-MO oocytes compared with that in the control oocytes (control-MO 25.99±1.27%, n=87, versus KIFC1-MO 56.99±4.26%, n=84, P<0.05) (Fig. 6F). The immunofluorescence intensity of Fmn2 was also significantly decreased (control-MO 1, n=109, versus KIFC1-MO 0.55±0.02, n=91, P<0.01) (Fig. 6G). Following Myc-KIFC1 mRNA injection, the protein expression of Fmn2 significantly recovered, which was confirmed by the band intensity analysis (control-MO 1, versus rescue 0.999, not significant; control-MO versus KIFC1-MO 0.332, P<0.01) (Fig. 6H). Spindle-periphery localized Fmn2 is required for spindle migration, and Fmn2 nucleates actin bundles from vesicles derived likely from the endoplasmic reticulum (ER) (Duan et al., 2020). We subsequently studied the effects

Development (2022) 149, dev200231. doi:10.1242/dev.200231

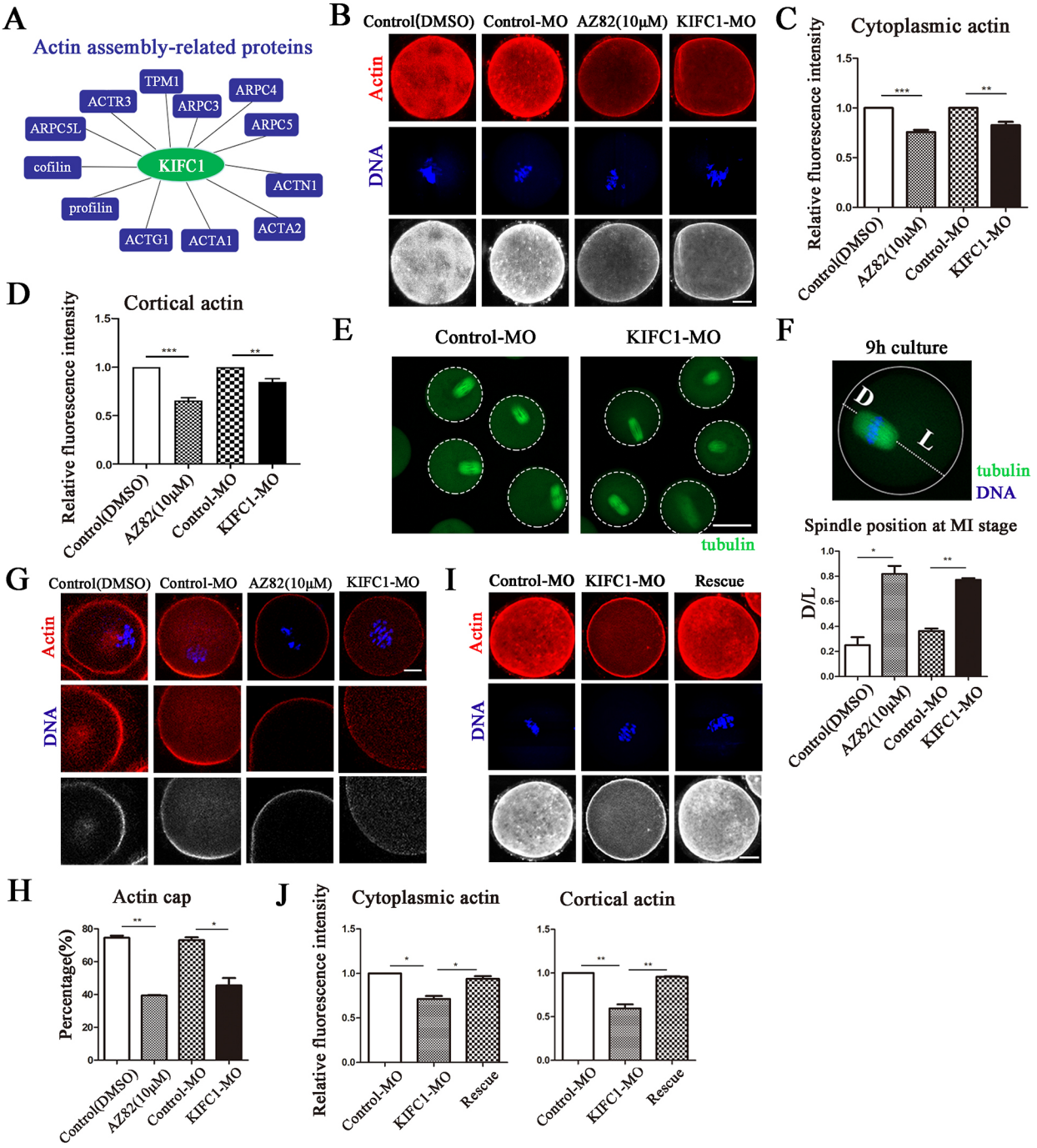

Fig. 5. KIFC1 regulates actin dynamics and spindle migration in mouse oocyte meiosis. (A) Screening actin-related proteins correlated with KIFC1 by mass spectrometry analysis. (B) Representative images of actin of metaphase I (MI) oocytes in control and treated groups. Actin and DNA are shown in red and blue, respectively. (C) KIFC1 suppression significantly decreased the fluorescence intensity of actin in the cytoplasm of MI-stage oocytes. (D) The actin fluorescence intensity in the cortex of MI-stage oocytes was significantly decreased in KIFC1 suppression group. (E) After culturing for 9 h, the spindle formed in the central cytoplasm and migrated to oocyte cortex in control oocytes. However, the spindle was still in the central cytoplasm in KIFC1-MO oocytes. Green, tubulin. (F) To quantitatively determine the spindle position in oocytes after KIFC1 suppression, we used the D/L ratio to measure spindle migration, which is marked in the fluorescence image. The value of D/L ratio in KIFC1 suppression groups was significantly higher than that in the control group. (G) KIFC1 suppression disturbed the formation of the actin cap during oocyte meiosis. Red, actin; blue, DNA. (H) Quantitative analysis of the proportion of actin cap formation in control and KIFC1 suppression oocytes. (I) Reduced fluorescence intensity of cytoplasmic and cortical actin in KIFC1-MO oocytes could be significantly rescued by Myc-KIFC1 mRNA injection. Red, actin; blue, DNA. (J) The fluorescence intensity of actin in the cytoplasm and cortex after Myc-KIFC1 mRNA injection was significantly increased compared with the KIFC1-MO group. Data are mean±s.e.m. **P*<0.05, ***P*<0.01, ****P*<0.001 (paired two-tailed Student's *t*-test). Scale bars: 20 µm (B,G,I); 100 µm (E).

of KIFC1 depletion on the ER, and ER of oocytes in the KIFC1-MO group was no longer evenly enriched around the functional spindles as seen in the control group (Fig. 6I). Quantitative analysis demonstrated that ER misdistribution was significantly increased in KIFC1-MO oocytes compared with that in the control oocytes (control-MO 31.78±0.79%, n=102, versus KIFC1-MO 59.66±3.17%, n=93, P<0.01) (Fig. 6J). These results suggested that KIFC1 regulated actin assembly and spindle

Development (2022) 149, dev200231. doi:10.1242/dev.200231

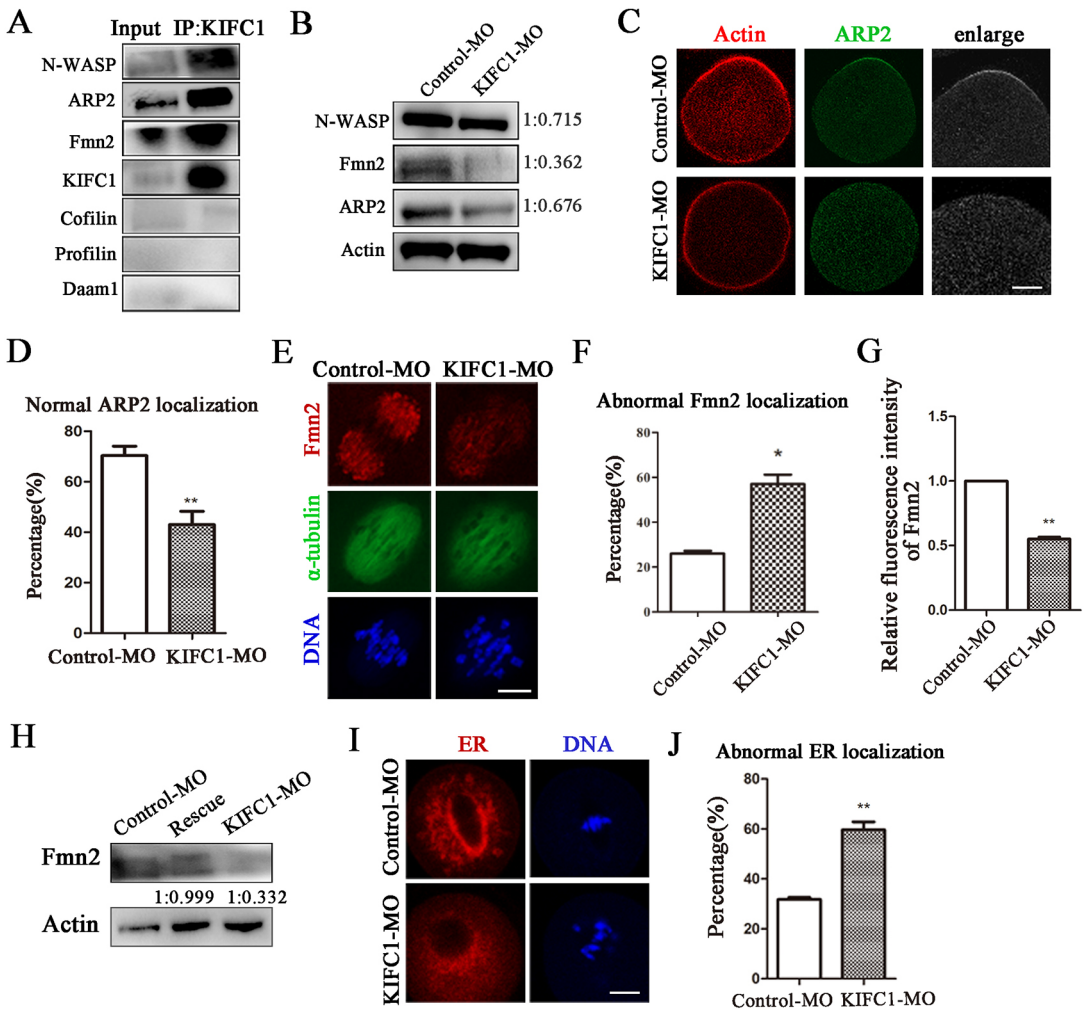

Fig. 6. KIFC1 regulates actin nucleator functions in mouse oocytes. (A) Co-IP results showed that KIFC1 was correlated with Fmn2, ARP2/3 complex and N-WASP, but not Daam1, cofilin and profilin. Mouse ovaries were lysed and subjected to IP with antibody, followed by western blot. (B) KIFC1 knockdown decreased the expression levels of Fmn2, ARP2 and N-WASP in MI-stage oocytes. (C) Representative images showing the distribution of ARP2 in control and KIFC1 suppression oocytes. Green, ARP2; red, actin. (D) Quantitative analysis of control and KIFC1 suppression oocytes with normal polarized distribution of ARP2. (E) Oocytes after KIFC1-MO injection displayed abnormal localization and reduced immunofluorescence signal of Fmn2. Red, Fmn2; green, tubulin; blue, DNA. (F) The rate of abnormal localization of Fmn2 was significantly increased in KIFC1-MO oocytes compared with that of the control oocytes. (G) The immunofluorescence intensity of Fmn2 was significantly decreased after KIFC1 knockdown. (H) The expression of Fmn2 was significantly recovered compared with the KIFC1 knockdown group after injection of Myc-KIFC1 mRNA. (I) Endoplasmic reticulum (ER) showed a disordered distribution after MO injection. Red, ER; blue, DNA. (J) The rate of ER misdistribution in the cytoplasm was significantly increased in KIFC1-MO oocytes compared with that of the control oocytes. Data are mean±s.e.m. **P*<0.05, ***P*<0.01 (paired two-tailed Student's *t*-test). Scale bars: 20 µm (C); 5 µm (E,I).

migration though Fmn2 and the ARP2/3 complex during mouse oocyte maturation.

DISCUSSION

KIFC1 has been reported to be functional on bipolar spindle formation in mitosis of different models (Tan et al., 2013). In the present study, we reported that in mouse oocyte meiosis, KIFC1 also acted on actin dynamics for spindle migration, indicating a previously unreported role of KIFC1 in the mouse oocyte meiosis model. Moreover, previous studies have mainly focused on actin nucleators for the actin-based mechanism of spindle migration, whereas our results showed that a kinesin motor could direct a microtubule-dependent mechanism for this process.

Kinesin proteins have important roles in microtubule dynamics, chromosome separation and cell cycle progression during both mitosis and meiosis. KIF25 is essential for maintaining spindle stability during Hela cell mitosis (Decarreau et al., 2017). KLP-7 (a member of the kinesin 13 family) is responsible for spindle organization and sister chromatid segregation in *Caenorhabditis elegans* embryos (Gigant et al., 2017). KLP-15/16, two highly homologous members of the kinesin-14 family, are present on the anaphase spindle and are essential for stabilizing the microtubule bundles (Mullen and Wignall, 2017). In mammalian female meiosis, KIF5B knockdown could induce the delay of GVBD and failure of polar body extrusion in mouse oocytes, and centrosome amplification/chromosomal segregation defect in mitotic cells (Kidane et al., 2013). MKlp2 (also called KIF20A) is involved in cytokinesis during meiotic maturation in both mouse oocytes and porcine oocytes (Liu et al., 2013; Zhang et al., 2014c). KIF1B is reported to affect spindle dynamics and mitochondria distribution in mouse oocytes and early embryos (Kong et al., 2016). KIFC1 also regulates microtubule nucleation and spindle assembly during mitosis (She and Yang, 2017). Our results showed that KIFC1 was essential for oocyte maturation:

Development (2022) 149, dev200231. doi:10.1242/dev.200231

inhibition of its activity or knockdown of its expression caused polar body extrusion defects. Previous studies have shown that bisphenol A (BPA) treatment caused the failure of oocyte maturation, whereas in this case KIFC1 showed lower expression along the spindle (Yang et al., 2020); moreover, in aged oocytes low expression of Kifc1 was observed and disruption of KIFC1 increased the aneuploidy (Mihalas et al., 2019). These all indicated the necessity of KIFC1 for oocyte maturation, and we showed that this might be because of the roles of KIFC1 on spindle assembly and chromosome alignment in mouse oocytes meiosis, which could be confirmed by the aberrant distribution of p-MAPK, a crucial regulator which is required for proper tubule nucleation and spindle formation during oocyte meiosis (Fan and Sun, 2004).

Ac-tubulin is present in various microtubule structures including the mitotic spindle, and is essential for microtubule stabilization and spindle formation (Chen et al., 2013). Altered acetylation level of tubulin leads to defective spindle assembly and chromosome misalignment in mouse oocyte meiosis (Lu et al., 2018). For example, inhibition of Kif11 activity downregulates the expression of ac-tubulin and further disturbs microtubule stability during porcine oocyte meiosis (Wan et al., 2018). During mouse oocyte maturation, both Kif4a (Kif4) and Kif18a knockdown disrupt spindle organization by affecting the acetylation levels of α-tubulin (Tang et al., 2018a,b). HDAC3 and NAT10 have been reported to affect microtubule stability by regulating tubulin acetylation in mouse oocytes (Larrieu et al., 2014; Li et al., 2017; Shen et al., 2009). HDAC6 is a microtubule deacetylase in mitotic and meiotic cells (Hubbert et al., 2002; Zhang et al., 2014a). Our results indicated that ac-tubulin level increased after knockdown or inhibition of KIFC1, and mass spectroscopy data indicated that some acetylation-related proteins were associated with KIFC1. Increased NAT10 (acetylation-related enzyme) and decreased HDAC6 (deacetylation-related enzymes) levels in KIFC1 knockdown oocytes were subsequently detected. Owing to the fact that KIFC1 shares the conserved functional domain with other kinesins, it is possible that KIFC1 functions in transporting the acetylases for tubulin acetylation in oocytes. Thus, these data suggested that NAT10 and HDAC6 might function downstream of KIFC1 for tubulin acetylation, which was essential for spindle organization and chromosome alignment in mouse oocytes.

In addition to its roles in tubulin acetylation on spindle organization, we found an interesting phenotype showing that KIFC1 suppression affected actin assembly, disturbed spindle migration and frustrated actin cap formation. Mass spectroscopy data showed that several crucial actin nucleation-related proteins such as N-WASP and the Arp2/3 complex were associated with KIFC1. Actin-based spindle migration from the oocyte center to a subcortical location and cytokinesis are indispensable for successful asymmetric meiotic cell division (Yi et al., 2013a). Crosstalk and integration between microtubules and actin microfilaments are fundamental for cell motility. DdKif5, known as the kinesin 1 isoform, appears to crosslink actin and integrates two cytoskeletal systems (Moen et al., 2011). The myosin also mediates crosstalk between microtubule and actin microfilament (Weber et al., 2004). MyoVa can efficiently maneuver its way through actin filament intersections and Arp2/3 branches. Furthermore, MyoVa is capable of coordinating kinesins with their cargos along microtubules (Ali et al., 2007). These studies indicate that kinesins may affect actin dynamics through microtubule-microfilament crosstalk during oocyte meiosis. Increasing studies show the roles of kinesins on actin regulation in meiosis. Pavarotti, a kinesin-like protein, binds directly to actin and has a vital role in regulating actin dynamics (Nakamura et al., 2020). Kif17 has ability to transport actin regulators RhoA-ROCK and modulate actin dynamics-related spindle migration during mouse oocyte meiosis (Wang et al., 2019). Kif14 is an actin-bundling kinesin to link microtubules with F-actin, which is important for cytokinesis in *Xenopus* oocytes (Samwer et al., 2013).

We next explored the regulatory mechanism of KIFC1 on actin assembly in oocytes, our co-IP results indicated that KIFC1 associated with both N-WASP-Arp2/3 and Fmn2, and functional experiments using knockdown and rescue approaches further confirmed our finding. In oocytes, several molecules such as the formin family, the Arp2/3 complex, RhoA-LIMK-cofilin and profilin are reported to regulate actin filament assembly (Duan and Sun, 2019). The N-WASP-ARP2/3 complex orchestrates actin polymerization-driven cytoplasmic streaming and spindle migration in mouse oocytes (Yi et al., 2013b). Spindle-periphery localized FMN2 is required for MI spindle migration, and it is dependent on the ability of F-actin nucleation (Li et al., 2008; Schuh and Ellenberg, 2008). Therefore, our data indicated that KIFC1 transported Arp2/3 and Fmn2 for actin nucleation in oocytes. Actin nucleators of the formin family are potential coordinators of the actin and microtubule cytoskeletons, as they can both nucleate actin filaments and bind microtubules *in vitro* (Chesarone et al., 2010). The spindle-peripheral FMN2 nucleates short actin bundles from vesicles derived from ER (Duan et al., 2020; Li et al., 2008). In the present study, we also showed that depletion of KIFC1 affected ER distribution, which indicated that KIFC1 might disrupt association of the ER with the spindle, which further affected the distribution of actin nucleators for actin-based spindle migration in mouse oocytes.

In conclusion, our results demonstrated that KIFC1 was important for microtubule acetylation-based spindle stability. Moreover, KIFC1 also played a previously unreported role in actin dynamics and spindle migration through ER-based Fmn2 and ARP2/3 function during mouse oocyte maturation (Fig. 7).

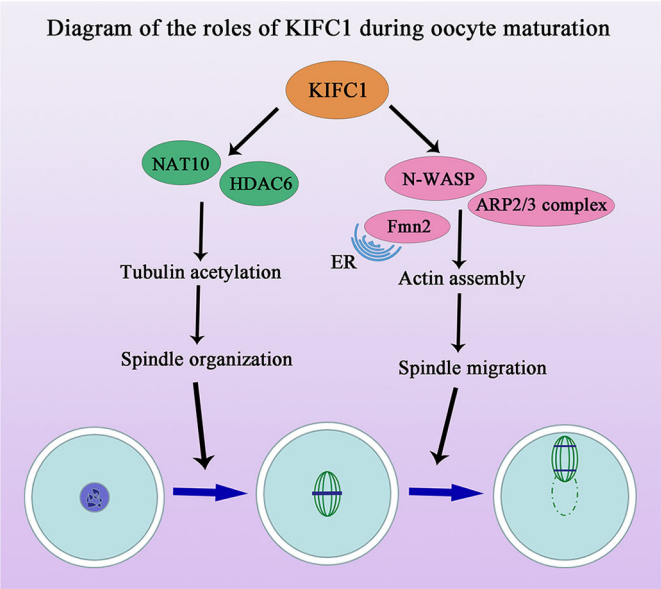

Fig. 7. Diagram of the roles of KIFC1 during mouse oocyte meiotic maturation. KIFC1 regulates tubulin acetylation by affecting the expression of HDAC6 and NAT10 for microtubule stability and spindle organization. Meanwhile, KIFC1 also modulates spindle migration by affecting endoplasmic reticulum (ER)-based Fmn2 and the ARP2/3 complex for actin assembly during mouse oocyte maturation.

Development (2022) 149, dev200231. doi:10.1242/dev.200231

MATERIALS AND METHODS

Antibodies and chemicals

KIFC1 inhibitor AZ82 (#hy-12241) was purchased from MedChemExpress. Rabbit polyclonal anti-KIFC1 antibody (#orb101014) was obtained from Biorbyt Explore Bioreagents and the rabbit polyclonal anti-phospho-p44/42 MAPK (Erk1/2), anti-α-tubulin antibodies (#2125S) were purchased from Cell Signaling Technology. The anti-NAT10 (#13365-a-AP) and anti-HDAC6 (#12834-1-AP) antibodies were purchased from Proteintech. Rabbit polyclonal anti-ARP2 antibody (#ab128934), anti-N-WASP antibody (#ab126626), anti-Fmn2 antibody (#ab72052), anti-cofilin antibody (#ab124979), anti-profilin antibody (#ab124904), anti-Daam1 antibody (#ab1221571) and anti-Myc antibody (#abab32072) were obtained from Abcam. Mouse anti-tubulin-FITC antibody (#F2168), anti-acetylated tubulin antibody (#T7451) and Hoechst 33342 were purchased from Sigma-Aldrich. Alexa Fluor 488 antibodies (A11008 or A11001) and the Alexa Fluor 594 antibodies (A11012 or A11005) were obtained from Invitrogen, and horseradish peroxidase-conjugated goat anti-rabbit/mouse antibodies (CW0103/CW0102) were obtained from CWBIO.

Collection and *in vitro* maturation of mice oocytes

All experiments were approved by the Animal Research Committee of Nanjing Agricultural University following the experimental animal committee guideline of Jiangsu Province (SYXK-Su-20170007). The mice were cared for in a 22°C temperature-controlled room with suitable light and fed with a lab mice maintenance diet. Mice were euthanized by cervical dislocation after ∼2-3 days housing. The immature oocytes displaying a clear GV were rapidly selected to culture in the M16 medium under paraffin oil at 37°C in a 5% CO_2 atmosphere. Oocytes were cultured and treated for analysis at the specific stages.

Nocodazole and taxol treatment of oocytes

For nocodazole treatment, 10 mg/ml nocodazole in DMSO stock was diluted in M16 medium (Sigma-Aldrich) to give a final concentration of 20 µg/ml. Oocytes were incubated in M16 medium supplemented with nocodazole for 10 min, and then after being cultured for 9 h were collected for immunofluorescence microscopy. For taxol treatment, oocytes at the metaphase I (MI) stage were incubated in M16 medium containing 10 µM taxol for 45 min.

AZ82 treatment

AZ82 is a KIFC1 inhibitor which can inhibit ATPase activity by peculiarly disturbing KIFC1-microtubule binding (Wu et al., 2013), and so was used to inhibit the biological activity of KIFC1. We tried different concentrations (6, 8 and 10 µM) of AZ82 for the oocyte culture, and 10 µM AZ82 was adopted due to the statistically significant difference of polar body extrusion rate. Samples in the control group were under 0.1% DMSO concentration in the culture medium to exclude the cytotoxicity on oocytes.

Plasmid construction and mRNA synthesis

Myc-KIFC1 vector was generated by Wuhan Gene Create Biological Engineering Co. We verified the results by sequencing and synthesizing mRNA from the plasmid linearized by AvrII using a HiScribe T7 High Yield RNA Synthesis Kit (New England Biolabs), capped with m7G (5′) ppp (5′) G (New England Biolabs) and tailed using a Poly(A) Polymerase Tailing Kit (Epicentre). mRNA was then purified with RNA Clean & Concentrator (Zymo Research) and saved at −80°C.

KIFC1 morpholino and mRNA injection

KIFC1-targeting morpholino antisense oligo (Gene Tools; 5′-TCCGCA-CAGAAAGGGTGCAAAGGCA-3′) was diluted with water to provide a working concentration of 1 mM according to the product instructions, and then ∼5-10 pl of oligo was microinjected into the cytoplasm of fully grown GV oocytes using a Narishige microinjector to knock down KIFC1 in mouse oocytes after incubation in the culture medium containing milrinone for 24 h. A nontargeting morpholino oligo (5′-CCTCTTACCTCAGTTA-CAATTTATA-3′) was injected as a control. For the rescue experiment, Myc-KIFC1 mRNA was injected into the oocytes at a concentration of 200 ng/µl 24 h after morpholino injection. After injection, the GV oocytes were cultured in M16 medium containing 1 µM milrinone for 4 h. Then, the oocytes were washed nine times in fresh M16 medium, and were transferred to fresh M16 medium for culture. The oocytes were cultured for subsequent experiments.

Immunofluorescence staining and confocal microscopy

Denuded oocytes were fixed with 4% paraformaldehyde/phosphate-buffered saline (PBS; pH 7.4) for 30 min and permeabilized in 0.1% Triton X-100 for 20 min at room temperature. After blocking with 1% bovine serum albumin-supplemented PBS for 1 h, oocytes were incubated with the primary antibodies (anti-KIFC1 1:100; anti-α-tubulin-FITC 1:200; anti-acetylated tubulin 1:200; anti-p-MAPK 1:200; anti-ARP2 1:100; anti-Fmn2 1:100; anti-Myc 1:100) at 4°C overnight. After washing with PBS containing 0.1% Tween 20 and 0.01% Triton X-100 three times (5 min each), oocytes were then transferred to appropriate fluorescent secondary antibody (1:200) in PBS for 1 h at room temperature. For Phalloidin staining, oocytes were incubated with Phalloidin-TRITC (5 µg/ml in PBS) for 1 h at room temperature. After washing three times again, all oocytes were counterstained with Hoechst-33342 (10 mg/ml in PBS) for 15 min at room temperature. Finally, the oocytes were mounted on glass slides and observed under a laser-scanning confocal fluorescent microscope (Zeiss LSM 700 META). We used live cell fluorescence staining to detect the distribution of ER (ER-Tracker Red, Beyotime). Oocytes were cultured at the appropriate stage, and then moved into M16 medium with fluorescent probes for 30 min and immediately imaged under the confocal microscopy.

Actin fluorescence intensity analysis

To measure actin fluorescence intensity, we set the same staining procedure indexes in the confocal microscope and acquired signals from oocytes in the control group and treatment group under coincident background. ImageJ was used to define a region of interest (ROI) of immunofluorescence in every image, and the average fluorescence intensity per unit area inside the ROI was determined. To measure cortical actin, the closed double-deck curvilinear rings were drawn along the cell membrane in oocytes of two groups, and the ROIs within the curved ring was determined. For the measurement of cytoplasmic actin intensity, we drew circles around the cytoplasm and determined the ROIs within the circles. The mean values of all measurements were used to compare the final average intensities between the control group and treatment group.

Mass spectroscopy analysis

We incubated 500 µl ovarian lysate with KIFC1 antibody and bead complexes, and the samples were then sent to the Wuhan Gene Create Biological Engineering Company for mass spectrometry (MS) analysis.

Co-immunoprecipitation and western blot

For co-IP, 800 oocytes were harvested in lysis buffer containing a protease inhibitor cocktail (CWBIO). A rabbit anti-KIFC1 monoclonal antibody was incubated overnight with the cell lysate and was subsequently incubated with Dynabeads Protein G (Thermo Fisher Scientific) for 5 h at 4°C. We then put the tube to a magnet. The immune complexes were next washed three times and were released from the beads by mixing in 2× SDS loading buffer for 20 min at 30°C. Samples were subsequently supplemented with NuPAGE LDS Sample Buffer (Thermo Fisher Scientific) and heated at 100°C for 10 min.

For western blotting, 250 mouse oocytes were collected and posited in SDS sample buffer and subsequently were rapidly frozen at −20°C after 5 min heating at 100°C. After being subjected to 12% SDS-PAGE, separated proteins were transferred to a PVDF membrane. Membranes were then blocked with PBST (containing 0.1% Tween 20 and 5% non-fat dry milk) for 1 h. Membranes were subsequently incubated with the following antibodies at 4°C overnight: rabbit monoclonal anti-KIFC1 (1:1000), rabbit monoclonal anti-α-tubulin (1:2000), mouse monoclonal anti-β-actin (1:2000, Cell Signaling Technology, #3700), rabbit monoclonal anti-ARP2 (1:1000), rabbit monoclonal anti-N-WASP (Ser616) (1:1000), rabbit polyclonal anti-ac-tubulin (1:1000), rabbit monoclonal anti-Fmn2 (1:1000), rabbit monoclonal anti-cofilin (1:1000), rabbit monoclonal anti-profilin

(1:1000), rabbit monoclonal anti-Daam1 (1:1000), rabbit monoclonal anti-Myc (1:1000), rabbit monoclonal anti-HDAC6 (1:1000), rabbit monoclonal anti-NAT10 (1:1000) and rabbit monoclonal anti-P-MAPK (1:1000). After washing three times (10 min each) with TBST (Tris-buffered saline with Tween 20), the membranes were incubated with a horseradish peroxidase-conjugated secondary antibody (1:10,000) at 37°C for 1 h. Protein band intensity was visualized using the ECL Plus Western Blotting Detection System (Tanon-5500). Band intensity values were terminally examined using ImageJ software to quantify western blot results.

Statistical analysis

All experiments were repeated at least three times. Group results were displayed as mean±s.e.m. Statistical analyses were performed using paired two-tailed Student's *t*-test with GraphPad Prism 5 software and are expressed as mean±s.e.m. $P<0.05$ was considered statistically significant.

Competing interests

The authors declare no competing or financial interests.

Author contributions

Conceptualization: M.-M.S., S.-C.S.; Methodology: M.-M.S., Y.-J.Z., H.-L.Z., Y.X., J.-Q.J.; Software: Y.-J.Z., Z.-N.P., H.-L.Z., Y.X., J.-Q.J.; Formal analysis: M.-M.S., S.-C.S.; Investigation: M.-M.S.; Resources: Y.-J.Z., Z.-N.P., H.-L.Z., Y.X., J.-Q.J.; Writing - original draft: M.-M.S.; Writing - review & editing: S.-C.S.; Supervision: S.-C.S.; Project administration: S.-C.S.; Funding acquisition: S.-C.S.

Funding

This work was supported by the National Natural Science Foundation of China (32170857) and the National Key Research and Development Program of China (2021YFC2700100).

Peer review history

The peer review history is available online at https://journals.biologists.com/dev/article-lookup/doi/10.1242/dev.200231.

References

Ali, M. Y., Krementsova, E. B., Kennedy, G. G., Mahaffy, R., Pollard, T. D., Trybus, K. M. and Warshaw, D. M. (2007). Myosin Va maneuvers through actin intersections and diffuses along microtubules. *Proc. Natl. Acad. Sci. USA* **104**, 4332-4336. doi:10.1073/pnas.0611471104

Azoury, J., Lee, K. W., Georget, V., Rassinier, P., Leader, B. and Verlhac, M.-H. (2008). Spindle positioning in mouse oocytes relies on a dynamic meshwork of actin filaments. *Curr. Biol.* **18**, 1514-1519. doi:10.1016/j.cub.2008.08.044

Braun, M., Drummond, D. R., Cross, R. A. and McAinsh, A. D. (2009). The kinesin-14 Klp2 organizes microtubules into parallel bundles by an ATP-dependent sorting mechanism. *Nat. Cell Biol.* **11**, 724-730. doi:10.1038/ncb1878

Cai, S., Weaver, L. N., Ems-McClung, S. C. and Walczak, C. E. (2009). Kinesin-14 family proteins HSET/XCTK2 control spindle length by cross-linking and sliding microtubules. *Mol. Biol. Cell* **20**, 1348-1359. doi:10.1091/mbc.e08-09-0971

Camlin, N. J., McLaughlin, E. A. and Holt, J. E. (2017a). Kif4 is essential for mouse oocyte meiosis. *PLoS ONE* **12**, e0170650. doi:10.1371/journal.pone.0170650

Camlin, N. J., McLaughlin, E. A. and Holt, J. E. (2017b). Motoring through: the role of kinesin superfamily proteins in female meiosis. *Hum. Reprod. Update* **23**, 409-420. doi:10.1093/humupd/dmx010

Chen, Y.-T., Chen, Y.-F., Chiu, W.-T., Liu, K.-Y., Liu, Y.-L., Chang, J.-Y., Chang, H.-C. and Shen, M.-R. (2013). Microtubule-associated histone deacetylase 6 supports the calcium store sensor STIM1 in mediating malignant cell behaviors. *Cancer Res.* **73**, 4500-4509. doi:10.1158/0008-5472.CAN-12-4127

Chesarone, M. A., DuPage, A. G. and Goode, B. L. (2010). Unleashing formins to remodel the actin and microtubule cytoskeletons. *Nat. Rev. Mol. Cell Biol.* **11**, 62-74. doi:10.1038/nrm2816

Coombes, C., Yamamoto, A., McClellan, M., Reid, T. A., Plooster, M., Luxton, G. W. G., Alper, J., Howard, J. and Gardner, M. K. (2016). Mechanism of microtubule lumen entry for the alpha-tubulin acetyltransferase enzyme alphaTAT1. *Proc. Natl. Acad. Sci. USA* **113**, E7176-E7184. doi:10.1073/pnas.1605397113

Decarreau, J., Wagenbach, M., Lynch, E., Halpern, A. R., Vaughan, J. C., Kollman, J. and Wordeman, L. (2017). The tetrameric kinesin Kif25 suppresses pre-mitotic centrosome separation to establish proper spindle orientation. *Nat. Cell Biol.* **19**, 384-390. doi:10.1038/ncb3486

Duan, X. and Sun, S.-C. (2019). Actin cytoskeleton dynamics in mammalian oocyte meiosis. *Biol. Reprod.* **100**, 15-24. doi:10.1093/biolre/ioy163

Duan, X., Liu, J., Dai, X.-X., Liu, H.-L., Cui, X.-S., Kim, N.-H., Wang, Z.-B., Wang, Q. and Sun, S.-C. (2014). Rho-GTPase effector ROCK phosphorylates cofilin in actin-meditated cytokinesis during mouse oocyte meiosis. *Biol. Reprod.* **90**, 37. doi:10.1095/biolreprod.113.113522

Duan, X., Li, Y., Yi, K., Guo, F., Wang, H., Wu, P. H., Yang, J., Mair, D. B., Morales, E. A., Kalab, P. et al. (2020). Dynamic organelle distribution initiates actin-based spindle migration in mouse oocytes. *Nat. Commun.* **11**, 277. doi:10.1038/s41467-019-14068-3

Endow, S. A. and Komma, D. J. (1997). Spindle dynamics during meiosis in *Drosophila* oocytes. *J. Cell Biol.* **137**, 1321-1336. doi:10.1083/jcb.137.6.1321

Fan, H.-Y. and Sun, Q.-Y. (2004). Involvement of mitogen-activated protein kinase cascade during oocyte maturation and fertilization in mammals. *Biol. Reprod.* **70**, 535-547. doi:10.1095/biolreprod.103.022830

Farina, F., Pierobon, P., Delevoye, C., Monnet, J., Dingli, F., Loew, D., Quanz, M., Dutreix, M. and Cappello, G. (2013). Kinesin KIFC1 actively transports bare double-stranded DNA. *Nucleic Acids Res.* **41**, 4926-4937. doi:10.1093/nar/gkt204

Fink, G., Hajdo, L., Skowronek, K. J., Reuther, C., Kasprzak, A. A. and Diez, S. (2009). The mitotic kinesin-14 Ncd drives directional microtubule-microtubule sliding. *Nat. Cell Biol.* **11**, 717-723. doi:10.1038/ncb1877

Gigant, E., Stefanutti, M., Laband, K., Gluszek-Kustusz, A., Edwards, F., Lacroix, B., Maton, G., Canman, J. C., Welburn, J. P. I. and Dumont, J. (2017). Inhibition of ectopic microtubule assembly by the kinesin-13 KLP-7 prevents chromosome segregation and cytokinesis defects in oocytes. *Development* **144**, 1674-1686. doi:10.1242/dev.147504

Hao, S.-L. and Yang, W.-X. (2019). KIFC1 is essential for normal spermatogenesis and its depletion results in early germ cell apoptosis in the Kuruma shrimp, Penaeus (Marsupenaeus) japonicus. *Aging (Albany NY)* **11**, 12773-12792. doi:10.18632/aging.102601

Hatsumi, M. and Endow, S. A. (1992). Mutants of the microtubule motor protein, nonclaret disjunctional, affect spindle structure and chromosome movement in meiosis and mitosis. *J. Cell Sci.* **101**, 547-559. doi:10.1242/jcs.101.3.547

Hentrich, C. and Surrey, T. (2010). Microtubule organization by the antagonistic mitotic motors kinesin-5 and kinesin-14. *J. Cell Biol.* **189**, 465-480. doi:10.1083/jcb.200910125

Hirokawa, N., Noda, Y., Tanaka, Y. and Niwa, S. (2009). Kinesin superfamily motor proteins and intracellular transport. *Nat. Rev. Mol. Cell Biol.* **10**, 682-696. doi:10.1038/nrm2774

Holubcová, Z., Howard, G. and Schuh, M. (2013). Vesicles modulate an actin network for asymmetric spindle positioning. *Nat. Cell Biol.* **15**, 937-947. doi:10.1038/ncb2802

Hubbert, C., Guardiola, A., Shao, R., Kawaguchi, Y., Ito, A., Nixon, A., Yoshida, M., Wang, X.-F. and Yao, T.-P. (2002). HDAC6 is a microtubule-associated deacetylase. *Nature* **417**, 455-458. doi:10.1038/417455a

Jang, J. K., Rahman, T., Kober, V. S., Cesario, J. and McKim, K. S. (2007). Misregulation of the kinesin-like protein Subito induces meiotic spindle formation in the absence of chromosomes and centrosomes. *Genetics* **177**, 267-280. doi:10.1534/genetics.107.076091

Kidane, D., Sakkas, D., Nottoli, T., McGrath, J. and Sweasy, J. B. (2013). Kinesin 5B (KIF5B) is required for progression through female meiosis and proper chromosomal segregation in mitotic cells. *PLoS ONE* **8**, e58585. doi:10.1371/journal.pone.0058585

Kong, X. W., Wang, D. H., Zhou, C. J., Zhou, H. X. and Liang, C. G. (2016). Loss of function of KIF1B impairs oocyte meiotic maturation and early embryonic development in mice. *Mol. Reprod. Dev.* **83**, 1027-1040. doi:10.1002/mrd.22744

Larrieu, D., Britton, S., Demir, M., Rodriguez, R. and Jackson, S. P. (2014). Chemical inhibition of NAT10 corrects defects of laminopathic cells. *Science* **344**, 527-532. doi:10.1126/science.1252651

Leader, B., Lim, H., Carabatsos, M. J., Harrington, A., Ecsedy, J., Pellman, D., Maas, R. and Leder, P. (2002). Formin-2, polyploidy, hypofertility and positioning of the meiotic spindle in mouse oocytes. *Nat. Cell Biol.* **4**, 921-928. doi:10.1038/ncb880

Li, H., Guo, F., Rubinstein, B. and Li, R. (2008). Actin-driven chromosomal motility leads to symmetry breaking in mammalian meiotic oocytes. *Nat. Cell Biol.* **10**, 1301-1308. doi:10.1038/ncb1788

Li, X., Liu, X., Gao, M., Han, L., Qiu, D., Wang, H., Xiong, B., Sun, S. C., Liu, H. and Gu, L. (2017). HDAC3 promotes meiotic apparatus assembly in mouse oocytes by modulating tubulin acetylation. *Development* **144**, 3789-3797. doi:10.1242/dev.153353

Liu, J., Wang, Q.-C., Cui, X.-S., Wang, Z.-B., Kim, N.-H. and Sun, S.-C. (2013). MKlp2 inhibitor paprotrain affects polar body extrusion during mouse oocyte maturation. *Reprod. Biol. Endocrinol.* **11**, 117. doi:10.1186/1477-7827-11-117

Lu, Y., Li, S., Cui, Z., Dai, X., Zhang, M., Miao, Y., Zhou, C., Ou, X. and Xiong, B. (2018). The cohesion establishment factor Esco1 acetylates alpha-tubulin to ensure proper spindle assembly in oocyte meiosis. *Nucleic Acids Res.* **46**, 2335-2346. doi:10.1093/nar/gky001

Magiera, M. M. and Janke, C. (2014). Post-translational modifications of tubulin. *Curr. Biol.* **24**, R351-R354. doi:10.1016/j.cub.2014.03.032

Mazumdar, M. and Misteli, T. (2005). Chromokinesins: multitalented players in mitosis. *Trends Cell Biol.* **15**, 349-355. doi:10.1016/j.tcb.2005.05.006

Mihalas, B. P., Camlin, N. J., Xavier, M. J., Peters, A. E., Holt, J. E., Sutherland, J. M., McLaughlin, E. A., Eamens, A. L. and Nixon, B. (2019).

The small non-coding RNA profile of mouse oocytes is modified during aging. *Aging (Albany NY)* **11**, 2968-2997. doi:10.18632/aging.101947

Moen, R. J., Johnsrud, D. O., Thomas, D. D. and Titus, M. A. (2011). Characterization of a myosin VII MyTH/FERM domain. *J. Mol. Biol.* **413**, 17-23. doi:10.1016/j.jmb.2011.08.036

Mullen, T. J. and Wignall, S. M. (2017). Interplay between microtubule bundling and sorting factors ensures acentriolar spindle stability during C. elegans oocyte meiosis. *PLoS Genet.* **13**, e1006986. doi:10.1371/journal.pgen.1006986

Nakamura, M., Verboon, J. M., Prentiss, C. L. and Parkhurst, S. M. (2020). The kinesin-like protein Pavarotti functions noncanonically to regulate actin dynamics. *J. Cell Biol.* **219**, e201912117. doi:10.1083/jcb.201912117

Pfender, S., Kuznetsov, V., Pleiser, S., Kerkhoff, E. and Schuh, M. (2011). Spire-type actin nucleators cooperate with Formin-2 to drive asymmetric oocyte division. *Curr. Biol.* **21**, 955-960. doi:10.1016/j.cub.2011.04.029

Samwer, M., Dehne, H.-J., Spira, F., Kollmar, M., Gerlich, D. W., Urlaub, H. and Görlich, D. (2013). The nuclear F-actin interactome of Xenopus oocytes reveals an actin-bundling kinesin that is essential for meiotic cytokinesis. *EMBO J.* **32**, 1886-1902. doi:10.1038/emboj.2013.108

Schuh, M. and Ellenberg, J. (2008). A new model for asymmetric spindle positioning in mouse oocytes. *Curr. Biol.* **18**, 1986-1992. doi:10.1016/j.cub.2008.11.022

She, Z.-Y. and Yang, W.-X. (2017). Molecular mechanisms of kinesin-14 motors in spindle assembly and chromosome segregation. *J. Cell Sci.* **130**, 2097-2110. doi:10.1242/jcs.200261

Shen, Q., Zheng, X., McNutt, M. A., Guang, L., Sun, Y., Wang, J., Gong, Y., Hou, L. and Zhang, B. (2009). NAT10, a nucleolar protein, localizes to the midbody and regulates cytokinesis and acetylation of microtubules. *Exp. Cell Res.* **315**, 1653-1667. doi:10.1016/j.yexcr.2009.03.007

Sirajuddin, M., Rice, L. M. and Vale, R. D. (2014). Regulation of microtubule motors by tubulin isotypes and post-translational modifications. *Nat. Cell Biol.* **16**, 335-344. doi:10.1038/ncb2920

Skold, H. N., Komma, D. J. and Endow, S. A. (2005). Assembly pathway of the anastral *Drosophila* oocyte meiosis I spindle. *J. Cell Sci.* **118**, 1745-1755. doi:10.1242/jcs.02304

Song, Y. and Brady, S. T. (2015). Post-translational modifications of tubulin: pathways to functional diversity of microtubules. *Trends Cell Biol.* **25**, 125-136. doi:10.1016/j.tcb.2014.10.004

Sun, S.-C., Wang, Z.-B., Xu, Y.-N., Lee, S.-E., Cui, X.-S. and Kim, N.-H. (2011). Arp2/3 complex regulates asymmetric division and cytokinesis in mouse oocytes. *PLoS ONE* **6**, e18392. doi:10.1371/journal.pone.0018392

Tan, F.-Q., Ma, X.-X., Zhu, J.-Q. and Yang, W.-X. (2013). The expression pattern of the C-terminal kinesin gene kifc1 during the spermatogenesis of Sepiella maindroni. *Gene* **532**, 53-62. doi:10.1016/j.gene.2013.09.008

Tang, F., Pan, M.-H., Lu, Y., Wan, X., Zhang, Y. and Sun, S.-C. (2018a). Involvement of Kif4a in spindle formation and chromosome segregation in mouse oocytes. *Aging Dis.* **9**, 623-633. doi:10.14336/AD.2017.0901

Tang, F., Pan, M.-H., Wan, X., Lu, Y., Zhang, Y. and Sun, S.-C. (2018b). Kif18a regulates Sirt2-mediated tubulin acetylation for spindle organization during mouse oocyte meiosis. *Cell Div* **13**, 9. doi:10.1186/s13008-018-0042-4

Wan, X., Zhang, Y., Lan, M., Pan, M.-H., Tang, F., Zhang, H.-L., Ou, X.-H. and Sun, S.-C. (2018). Meiotic arrest and spindle defects are associated with altered KIF11 expression in porcine oocytes. *Environ. Mol. Mutagen*. **59**, 805-812. doi:10.1002/em.22213

Wang, H.-H., Zhang, Y., Tang, F., Pan, M.-H., Wan, X., Li, X.-H. and Sun, S.-C. (2019). Rab23/Kif17 regulate meiotic progression in oocytes by modulating tubulin acetylation and actin dynamics. *Development* **146**, dev171280. doi:10.1242/dev.171280

Weber, K. L., Sokac, A. M., Berg, J. S., Cheney, R. E. and Bement, W. M. (2004). A microtubule-binding myosin required for nuclear anchoring and spindle assembly. *Nature* **431**, 325-329. doi:10.1038/nature02834

Wu, J., Mikule, K., Wang, W., Su, N., Petteruti, P., Gharahdaghi, F., Code, E., Zhu, X., Jacques, K., Lai, Z. et al. (2013). Discovery and mechanistic study of a small molecule inhibitor for motor protein KIFC1. *ACS Chem. Biol.* **8**, 2201-2208. doi:10.1021/cb400186w

Yang, L., Baumann, C., De La Fuente, R. and Viveiros, M. M. (2020). Mechanisms underlying disruption of oocyte spindle stability by bisphenol compounds. *Reproduction* **159**, 383-396. doi:10.1530/REP-19-0494

Yi, K., Unruh, J. R., Deng, M., Slaughter, B. D., Rubinstein, B. and Li, R. (2011). Dynamic maintenance of asymmetric meiotic spindle position through Arp2/3-complex-driven cytoplasmic streaming in mouse oocytes. *Nat. Cell Biol.* **13**, 1252-1258. doi:10.1038/ncb2320

Yi, K., Rubinstein, B. and Li, R. (2013a). Symmetry breaking and polarity establishment during mouse oocyte maturation. *Philos. Trans. R. Soc. Lond. B Biol. Sci.* **368**, 20130002. doi:10.1098/rstb.2013.0002

Yi, K., Rubinstein, B., Unruh, J. R., Guo, F., Slaughter, B. D. and Li, R. (2013b). Sequential actin-based pushing forces drive meiosis I chromosome migration and symmetry breaking in oocytes. *J. Cell Biol.* **200**, 567-576. doi:10.1083/jcb.201211068

Yi, Z.-Y., Ma, X.-S., Liang, Q.-X., Zhang, T., Xu, Z.-Y., Meng, T.-G., Ouyang, Y.-C., Hou, Y., Schatten, H., Sun, Q.-Y. et al. (2016). Kif2a regulates spindle organization and cell cycle progression in meiotic oocytes. *Sci. Rep.* **6**, 38574. doi:10.1038/srep38574

Zhang, L., Hou, X., Ma, R., Moley, K., Schedi, T. and Wang, Q. (2014a). Sirt2 functions in spindle organization and chromosome alignment in mouse oocyte meiosis. *FASEB J.* **28**, 1435-1445. doi:10.1096/fj.13-244111

Zhang, Y., Duan, X., Cao, R., Liu, H.-L., Cui, X.-S., Kim, N.-H., Rui, R. and Sun, S.-C. (2014b). Small GTPase RhoA regulates cytoskeleton dynamics during porcine oocyte maturation and early embryo development. *Cell Cycle* **13**, 3390-3403. doi:10.4161/15384101.2014.952967

Zhang, Y., Liu, J., Peng, X., Zhu, C.-C., Han, J., Luo, J. and Rui, R. (2014c). KIF20A regulates porcine oocyte maturation and early embryo development. *PLoS ONE* **9**, e102898. doi:10.1371/journal.pone.0102898

Zhi, E., Li, P., Chen, H., Xu, P., Zhu, X., Zhu, Z., He, Z. and Li, Z. (2016). Decreased expression of KIFC1 in human testes with globozoospermic defects. *Genes (Basel)* **7**, 75. doi:10.3390/genes7100075